

# Neural Stereo Video Compression with Hybrid Disparity Compensation

Shiyin Jiang<sup>1</sup>, Zhenghao Chen<sup>2</sup>, Minghao Han<sup>1</sup>, Xingyu Zhou<sup>1</sup>, Leheng Zhang<sup>1</sup>, Shuhang Gu<sup>1\*</sup>

<sup>1</sup>University of Electronic Science and Technology of China

<sup>2</sup>The University of Newcastle, Australia

{shiyin.jsy, shuhanggu}@gmail.com, zhenghao.chen@newcastle.edu.au

## Abstract

*Disparity compensation represents the primary strategy in stereo video compression (SVC) for exploiting cross-view redundancy. These mechanisms can be broadly categorized into two types: one that employs explicit horizontal shifting, and another that utilizes an implicit cross-attention mechanism to reduce cross-view disparity redundancy. In this work, we propose a hybrid disparity compensation (HDC) strategy that leverages explicit pixel displacement as a robust prior feature to simplify optimization and perform implicit cross-attention mechanisms for subsequent warping operations, thereby capturing a broader range of disparity information. Specifically, HDC first computes a similarity map by fusing the horizontally shifted cross-view features to capture pixel displacement information. This similarity map is then normalized into an “explicit pixel-wise attention score” to perform the cross-attention mechanism, implicitly aligning features from one view to another. Building upon HDC, we introduce a novel end-to-end optimized neural stereo video compression framework, which integrates HDC-based modules into key coding operations, including cross-view feature extraction and reconstruction (HDC-FER) and cross-view entropy modeling (HDC-EM). Extensive experiments on SVC benchmarks, including KITTI 2012, KITTI 2015, and Nagoya, which cover both autonomous driving and general scenes, demonstrate that our framework outperforms both neural and traditional SVC methodologies.*

## 1. Introduction

As stereoscopic cameras become increasingly common in newly launched smart products, such as virtual reality headsets and autonomous vehicles, the demand for efficient storage and transmission of large volumes of stereo video is growing. Stereo video compression (SVC) [11, 25, 53, 55] has recently gained significant attention for its ability to en-

code stereo videos into compact bitstreams, reducing both storage and transmission costs.

A key challenge in this task is reducing cross-view redundancy, and disparity compensation is central to this effort. By aligning stereo views, disparity compensation enables the extraction of missing details and the reuse of shared information, which enhances reconstruction quality and improves compression efficiency. Traditional stereo video codecs [53, 55] rely on handcrafted disparity compensation methods, but these approaches are limited by the constraints of manually designed structures. The recent success of deep neural networks (DNNs) in stereo visual data processing [15, 20, 29, 49, 56, 57, 65] has paved the way for neural-based disparity compensation mechanisms. These modern techniques offer a more flexible and accurate solution for reducing cross-view redundancy in stereo video compression.

Existing neural-based disparity compensation methods can be classified into two categories. The first category leverages explicit disparity information to align cross-view features. This information is typically derived from standard operations such as varying disparity shifts [25, 38, 60], predicted disparity shifts [25, 64], or a homography matrix [17]. Incorporating these explicit operations provides a clear structural prior with direct geometric guidance, thereby simplifying optimization. However, while this approach reduces the complexity of the search space by predominantly focusing on local pixel neighborhoods, its reliance on local feature matching can limit robustness in occluded regions and may lead to erroneous matches. On the other hand, another category produces implicit disparity information by applying a cross-attention mechanism across both views to generate an implicit similarity map [31, 61, 66]. Leveraging global matching, this approach dynamically aggregates cross-view features based on attention maps, thereby extending its range and better addressing corner cases such as noises and occlusions. However, the global matching operation required to produce the similarity map is typically harder to optimize and computationally more expensive than directly generating pixel dis-

\*Corresponding author.

placement, resulting in slower convergence, increased training overhead, and greater optimization difficulty.

In this work, we introduce a hybrid disparity compensation (HDC) strategy that leverages the simplicity of explicit pixel displacement as a robust prior for straightforward optimization while harnessing the high performance of implicit cross-attention mechanisms for effective disparity compensation. Specifically, HDC begins by applying horizontal shifts to the features from both perspectives, generating two feature volumes corresponding to different disparity shifts. An element-wise dot product between these feature volumes computes a similarity map, which is normalized to produce an “attention score”. This score is then used in a cross-attention mechanism for each view, implicitly aligning the projected information from one view to the other to complete the disparity compensation process. Compared to conventional explicit compensation algorithms, our approach facilitates a more flexible search for disparity compensation by leveraging the dynamic nature of the attention score to encompass broader ranges. Additionally, our method streamlines the optimization process relative to implicit compensation techniques by employing standard operations (*i.e.*, shifting) to extract cross-view disparity information, thereby providing a structural prior that enhances neural network learning.

Building upon HDC, we propose a novel end-to-end optimized neural stereo video compression (NSVC) framework that integrates HDC-based modules into key coding operations: cross-view feature extraction and reconstruction (HDC-FER) and cross-view entropy modeling (HDC-EM). Specifically, HDC-FER extracts and reconstructs enhanced cross-view features by aligning features from one view to another, thereby integrating information from both views to facilitate the encoding and decoding of each specific view. Additionally, HDC-EM improves the contexture coding procedure by partitioning the quantized latent features from each view into sub-quantized latent features along the channel dimension and then progressively and iteratively entropy encoding them. In this process, previously encoded sub-quantized latent features from both views are used as priors, and the HDC mechanism aligns sub-features from another view to the current coding feature, thereby refining these priors.

We conduct extensive experiments to evaluate our framework on widely used automotive stereo video benchmarks, including KITTI 2012 [19] and KITTI 2015 [46]. In contrast to previous NSVC methods [11, 25]—which have been evaluated solely on automotive scenes—we also test our approach on general multi-view scenes using the Nagoya dataset [3], a standard stereo video benchmark in MV-HEVC [53, 55]. The results indicate that our framework outperforms both neural and traditional SVC methods in both automotive and general scenes. Our contributions can

be summarized as follows:

- We propose a hybrid disparity compensation (HDC) strategy that leverages explicit pixel displacement as a robust disparity prior to streamline optimization while incorporating implicit cross-attention mechanisms for improved compensation performance.
- We develop an end-to-end optimized NSVC framework by integrating our HDC into key components, including cross-view feature extraction and reconstruction (HDC-FER) and cross-view entropy modeling (HDC-EM).
- Extensive experiments demonstrate that our framework outperforms existing SVC methods on the benchmarks covering both autonomous driving and general scenes.

## 2. Related Work

### 2.1. Single-view Image and Video Compression

Single-view image and video compression eliminates spatial and temporal redundancies to achieve efficient encoding with minimal information loss. Traditional image codecs [7, 9, 51] rely on hand-crafted transforms (*e.g.*, DCT) to remove spatial redundancy, while video codecs [9, 52, 59] use motion compensation to leverage content from previous frames. Despite their effectiveness, these manually designed approaches have fundamental limitations in optimizing compression efficiency.

Learning-based methods overcome these constraints by optimizing compression end-to-end. Ballé et al. [5] introduced a neural transform coding framework for image compression, significantly improving coding efficiency. Building on this, subsequent works [6, 10, 14, 21–23, 32, 39–41, 47, 62, 67] enhanced entropy models and network architectures, surpassing traditional codecs. In video compression, Lu et al. [43] pioneered the first neural video codec (DVC) by integrating learnable motion compensation into a neural image compression framework. Following this, research efforts [4, 12, 13, 18, 24, 26–28, 33–37, 45, 50] have progressively improved motion estimation, compensation mechanisms, and entropy models, leading to steady advancements in compression performance.

### 2.2. Stereo Image and Video Compression

Stereo image and video compression extends single-view methods by addressing cross-view redundancy through disparity compensation, which aligns stereo views to enhance reconstruction and compression efficiency. Traditional methods such as MV-HEVC [53] augment HEVC [52] with handcrafted disparity compensation but struggle to fully exploit cross-view dependencies.

Recent advances in deep learning for stereo vision [15, 20, 29, 49, 56, 57, 65] have led to more flexible disparity compensation techniques. In stereo image compression, explicit methods leverage predefined disparity shifts or transformations for feature alignment [17, 38, 60], while

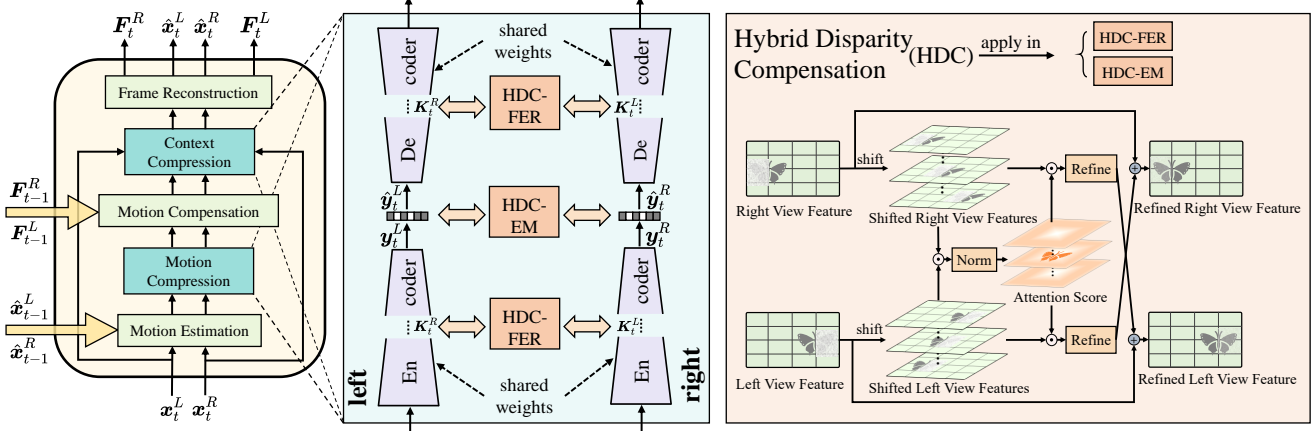


Figure 1. The overall architecture of the proposed framework. At time step  $t$ , the input frame pair  $\{\mathbf{x}_t^L, \mathbf{x}_t^R\}$  is compressed by a series of modules, conditioned on the reconstructed frame pair  $\{\hat{\mathbf{x}}_{t-1}^L, \hat{\mathbf{x}}_{t-1}^R\}$  and feature pair  $\{\mathbf{F}_t^L, \mathbf{F}_t^R\}$  from the previous time step. In particular, the proposed **HDC-FER** and **HDC-EM** modules, which extend our hybrid disparity compensation (**HDC**) strategy to feature extraction and reconstruction, as well as entropy modeling, are integrated into both the motion and context compression components to reduce cross-view redundancy during the encoder-decoder transform and entropy prediction processes.

implicit methods employ cross-attention for feature fusion [42, 61, 66], both of which significantly improve compression performance.

For stereo video compression, neural stereo video codecs (NSVCs) are also designed to eliminate cross-view redundancy. LSVC [11] sequentially compresses each view using offset-based disparity compensation, whereas LLSS [25] builds a cost volume with a *Bishift* operation, enabling parallel compression while capturing more comprehensive disparity information.

Broadly, existing disparity compensation techniques fall into two categories. Explicit alignment methods [11, 17, 25, 38, 60, 64] use predefined disparity shifts for feature warping, providing strong geometric guidance. However, they primarily focus on local pixel correspondences, making them less effective in occluded regions or when disparity estimates deviate from assumed shifts. In contrast, implicit alignment methods [31, 61, 66] employ cross-attention to perform global feature matching, which enhances robustness against occlusions and noise. Nevertheless, this approach comes with increased computational complexity and training challenges, often leading to slower convergence. By integrating both alignment strategies, our proposed hybrid disparity compensation (HDC) strategy combines the geometric reliability of explicit shifts with the adaptability of cross-attention, enabling more efficient and robust stereo video compression.

### 3. Methodology

### 3.1. Overall Architecture

Given a stereo frame pair  $\{x_t^L, x_t^R\}$  at time step  $t$ , the goal of NSVC is to represent this frame pair  $\{x_t^L, x_t^R\}$

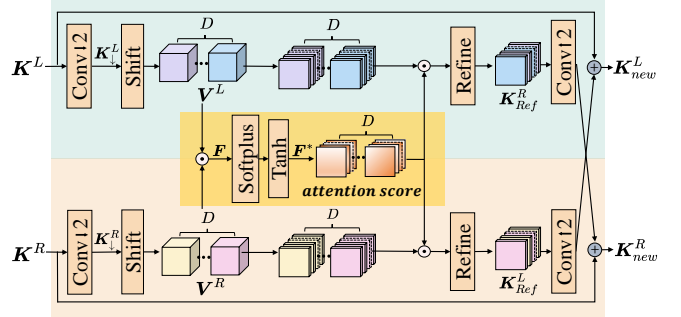


Figure 2. The proposed hybrid disparity compensation module for feature extraction and reconstruction (**HDC-FER**). Given input features  $\mathbf{K}^L$  and  $\mathbf{K}^R$ , 4D volumes  $\mathbf{V}^L$  and  $\mathbf{V}^R$  are generated by downsampling and shifting  $\mathbf{K}^L$  and  $\mathbf{K}^R$  [25, 29, 49], along the width dimension ( $W$ ) from 1 to  $D$ .  $D$  is the max disparity value. An attention score  $\mathbf{F}^*$  is then generated to weight and fuse the 4D volumes, producing aligned reference features  $\mathbf{K}_{Ref}^R$  and  $\mathbf{K}_{Ref}^L$  to enhance  $\mathbf{K}^R$  and  $\mathbf{K}^L$ .

with fewer bits through an encoding process, with the original format can be restored via a reverse decoding process, while maintaining a specified level of reconstruction quality. In this paper, we propose an enhanced stereo video codec that builds upon modified video compression framework DCVC-TCM [50] to compress stereo video frames, an overview of our framework can be found in the left part of Fig. 1. With the input stereo frame pair  $\{x_t^L, x_t^R\}$  at time step  $t$ , motion vector pair  $\{mv_t^L, mv_t^R\}$  is initially estimated by the motion estimation network, using the reconstructed frame pair  $\{\hat{x}_{t-1}^L, \hat{x}_{t-1}^R\}$  from time step  $t-1$ . The estimated motion vector is then compressed by the motion

compression network and reconstructed as  $\{\hat{\mathbf{mv}}_t^L, \hat{\mathbf{mv}}_t^R\}$ . Subsequently, the motion compensation network generates multi-scale context features for each view using the feature pair  $\{\mathbf{F}_{t-1}^L, \mathbf{F}_{t-1}^R\}$  from the previous time step, and utilizes  $\{\hat{\mathbf{mv}}_t^L, \hat{\mathbf{mv}}_t^R\}$  to align the multi-scale context features to the current time step, producing an aligned multi-scale context feature pair  $\{\mathbf{Ctx}_{1\sim 3}^L, \mathbf{Ctx}_{1\sim 3}^R\}$ . Following this,  $\{\mathbf{x}_t^L, \mathbf{x}_t^R\}$  is compressed by the context compression network, and reconstructed as  $\{\mathbf{F}_t^L, \mathbf{F}_t^R\}$ , with  $\{\mathbf{Ctx}_{1\sim 3}^L, \mathbf{Ctx}_{1\sim 3}^R\}$  serving as conditional input. Finally, the reconstructed feature pair  $\{\mathbf{F}_t^L, \mathbf{F}_t^R\}$  is fed into the frame reconstruction network to obtain the reconstructed frame pair  $\{\hat{\mathbf{x}}_t^L, \hat{\mathbf{x}}_t^R\}$ . Among the above five components, the motion estimation and motion compensation components mainly exploit temporal information to reduce transmission bit-stream, while the frame reconstruction component is a general module of reconstructing high quality image from processed feature. In this paper, we reduce cross-view redundancy in both the frame pair  $\{\mathbf{x}_t^L, \mathbf{x}_t^R\}$  and motion vector pair  $\{\mathbf{mv}_t^L, \mathbf{mv}_t^R\}$  by introducing the **Hybrid Disparity Compensation** (HDC) strategy. HDC is incorporated into both the **Motion Compression** and **Context Compression** modules to improve compression efficiency and reduce stereo video transmission overhead.

To achieve this, HDC integrates explicit pixel displacement, which provides a robust structural prior, with implicit cross-attention mechanisms for effective disparity compensation. As illustrated in the right part of Fig. 1, HDC first horizontally shifts features from both views to construct feature volumes at different disparity levels. A similarity map is then computed via an element-wise dot product between these volumes, followed by normalization to generate an attention score. This score is subsequently used in a cross-attention mechanism to adaptively align features across views, enabling efficient cross-view feature fusion.

Building on the HDC strategy, we introduce two HDC-based modules: Hybrid Disparity Compensation for Feature Extraction and Reconstruction (HDC-FER) and Hybrid Disparity Compensation for Entropy Modeling (HDC-EM). HDC-FER leverages the HDC mechanism to align and fuse cross-view features during feature extraction and reconstruction, thereby enhancing the quality of the recovered features. In contrast, HDC-EM incorporates aligned cross-view features as prior information during autoregressive entropy modeling to improve entropy prediction. Detailed descriptions of HDC-FER and HDC-EM are provided in Sec. 3.2.1 and Sec. 3.2.2.

### 3.2. Integration of HDC in our NSVC

#### 3.2.1. HDC for Feature Extraction and Reconstruction

In NSVCs, the encoder and decoder serve crucial roles in transforming the raw input and its latent representation into each other, effectively handling feature extraction and

reconstruction. A sophisticated latent representation not only reconstructs the input with high fidelity but also remains amenable to compression, underscoring the importance of advanced encoder-decoder architectures in neural-based compression models. In this subsection, we explain how our Hybrid Disparity Compensation module for Feature Extraction and Reconstruction (HDC-FER) leverages cross-view information in features of both views to produce more informative features, thereby enhancing stereo video compression efficiency.

Our HDC-FER module is designed to enhance feature representation during feature extraction and reconstruction by leveraging HDC-based cross-view alignment. Specifically, HDC-FER performs bidirectional alignment, mapping features from each view to its counterpart, enabling mutual enhancement and improving stereo video compression efficiency. For simplicity, we denote the intermediate features of the left view and right view in the encoder-decoder as  $\mathbf{K}^L$  and  $\mathbf{K}^R$ , respectively (see Fig. 2). Since there exists a significant disparity offset along the width dimension between  $\mathbf{K}^L$  and  $\mathbf{K}^R$ , it is hard for the convolutional networks to aggregate cross-view information for the two views due to a limited receptive field. To address this, we follow prior stereo-processing works [25, 29, 49] and shift feature maps horizontally from 1 to a maximum disparity value, constructing 4D feature volumes  $\mathbf{V}^L$  and  $\mathbf{V}^R$  with the shape of  $D \times C \times H \times W$ :

$$\begin{aligned} \mathbf{V}^L(d, c, h, w) &= \mathbf{K}_{\downarrow}^L(c, h, w + d), \\ \mathbf{V}^R(d, c, h, w) &= \mathbf{K}_{\downarrow}^R(c, h, w - d), \end{aligned} \quad (1)$$

where  $C$ ,  $H$  and  $W$  denote the number of channels, height, and width of the feature maps, and the corresponding lowercase letters are their respective indices;  $\mathbf{K}_{\downarrow}^L$  and  $\mathbf{K}_{\downarrow}^R$  are the downsampled intermediate feature maps as shown in Fig. 2. Next, we compute a cross-view similarity map using an element-wise dot product between the feature volumes:

$$\mathbf{F} = \mathbf{V}^L \odot \mathbf{V}^R. \quad (2)$$

This similarity map  $\mathbf{F}$  is then normalized using the Softplus and Tanh functions, inspired by the Mish activation function [48], to suppress irrelevant values and enhance significant correlations. The resulting attention score  $\mathbf{F}^*$  serves as a disparity-aware cross-view similarity measure, indicating how well features at different disparity shifts correspond across views. To aggregate aligned cross-view features, we employ a cross-attention mechanism using a weighted soft-warp operation. Specifically, we perform a 3D convolution over the weighted feature volumes to obtain reference features  $\mathbf{K}_{\text{Ref}}^L$  and  $\mathbf{K}_{\text{Ref}}^R$ :

$$\begin{aligned} \mathbf{K}_{\text{Ref}}^L &= \text{Conv3D}(\mathbf{F}^* \odot \mathbf{V}^R), \\ \mathbf{K}_{\text{Ref}}^R &= \text{Conv3D}(\mathbf{F}^* \odot \mathbf{V}^L), \end{aligned} \quad (3)$$

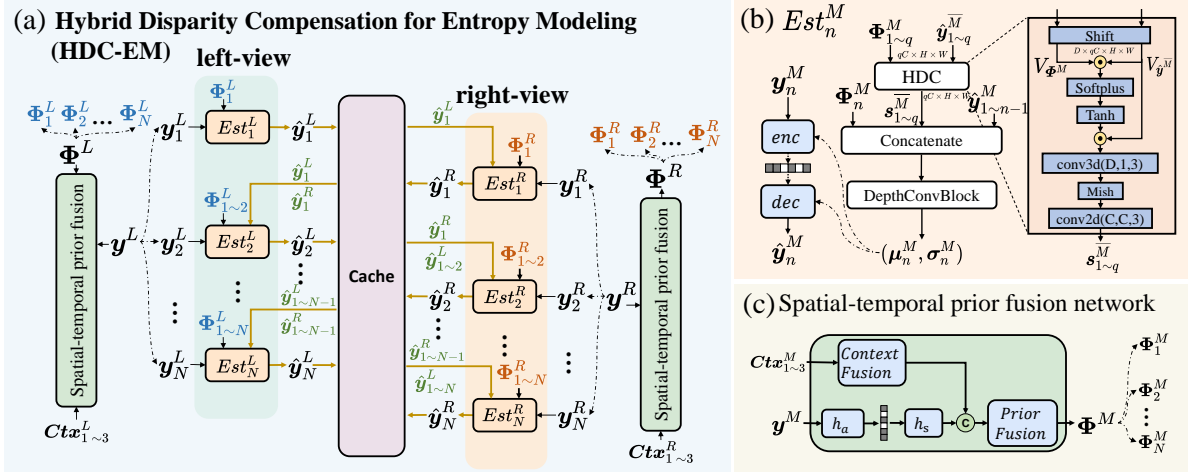


Figure 3. (a) The proposed Hybrid Disparity Compensation for Entropy Modeling (HDC-EM). The latent features  $y^L$  and  $y^R$ , extracted by the encoder (see Fig. 1), are divided into  $N$  equal slices along the channel dimension. These slices are processed autoregressively by the entropy estimation network  $Est_n^M$  ( $n \in \{1, \dots, N\}$ , where  $M$  denotes the left or right view) to generate coding symbols  $\{\hat{y}_1^L, \dots, \hat{y}_N^L\}$  and  $\{\hat{y}_1^R, \dots, \hat{y}_N^R\}$ . Here,  $Ctx_{1\sim 3}^M$  represents the multi-scale context features described in Sec. 3.1; (b) The entropy estimation network  $Est_n^M$  predicts the probability distribution for each latent slice  $\hat{y}_n^M$  using a context that comprises intra-view slices  $\hat{y}_{1\sim n-1}^M$ , cross-view slices  $\hat{y}_{1\sim n-1}^{\bar{M}}$  (aligned to the current view via the HDC mechanism, with  $q = n - 1$  for the left view and  $q = n$  for the right view), and spatial-temporal slices  $\Phi_{1\sim n}^M$ . The coding symbol  $\hat{y}_n^M$  is then generated and encoded using the predicted mean  $\mu_n^M$  and scale  $\sigma_n^M$ ; (c) The spatial-temporal prior fusion network generates the context  $\Phi^M$  by fusing the hyperprior—extracted from  $y^M$  via the hyper encoder-decoder ( $h_a$  and  $h_s$ )—with the multi-scale context features  $Ctx_{1\sim 3}^M$ . The fused context is then evenly divided into  $N$  slices to support entropy prediction. (Note: In the motion compression module, the context fusion network is omitted.)

These reference features undergo upsampling and are added to the original inputs, enabling each view to enhance its feature representation using complementary information from the other view. Thus, HDC-FER integrates the HDC-based cross-attention mechanism into feature extraction and reconstruction, ensuring that each view benefits from the most relevant cross-view features. This results in a more informative and compact latent representation, improving stereo video compression efficiency.

### 3.2.2. HDC for Cross-View Entropy Modeling

In stereo video compression, entropy modeling refers to modeling the probability distribution of latent features for arithmetic coding (the lossless compression stage of a codec). A more accurate entropy model yields a better estimate of the latent feature distribution, thereby reducing the required bitstream size. In this work, we propose a Hybrid Disparity Compensation for Cross-View Entropy Modeling (HDC-EM) module to improve entropy prediction accuracy by exploiting cross-view correlations. HDC-EM enhances context-based entropy coding by partitioning quantized latent features of each view into multiple channel-wise slices for progressive encoding. During this progressive encoding, previously encoded latent features from both views serve as priors. The HDC mechanism aligns the opposite view's features to the current view, refining these cross-view priors. This cross-view alignment provides more informative pri-

ors for the entropy model, enabling more accurate probability predictions and ultimately more efficient compression.

Without loss of generality, let  $y^L$  and  $y^R$  denote the latent representations produced by the encoder for the left and right views, respectively, and let  $\hat{y}^L$  and  $\hat{y}^R$  be their quantized forms (coding symbols). Following recent channel-wise entropy modeling approaches in learned image compression [14, 23, 39], we evenly partition  $y^L$  and  $y^R$  along the channel dimension into  $N$  slices (see Fig. 3 (a):  $\{y_1^L, y_2^L, \dots, y_N^L\}$  and  $\{y_1^R, y_2^R, \dots, y_N^R\}$ ). These slices are then encoded sequentially (slice by slice), yielding corresponding quantized slices  $\{\hat{y}_1^L, \hat{y}_2^L, \dots, \hat{y}_N^L\}$  and  $\{\hat{y}_1^R, \hat{y}_2^R, \dots, \hat{y}_N^R\}$ . To leverage inter-view dependencies, the encoding follows an alternating order between the two views:

$$\hat{y}_1^L \rightarrow \hat{y}_1^R \rightarrow \hat{y}_2^L \rightarrow \hat{y}_2^R \rightarrow \dots \rightarrow \hat{y}_N^L \rightarrow \hat{y}_N^R. \quad (4)$$

In this progressive coding scheme, each new slice's entropy modeling is conditioned on previously encoded information. Specifically, for slice  $y_n^M$  (where  $M \in \{L, R\}$ , denotes the current view and  $\bar{M}$  denotes the opposite view), the entropy estimation network  $Est_n^M$  integrates three types of priors to predict the probability distribution of the quantized slice  $\hat{y}_n^M$ . First, *intra-view priors*, which include previously encoded slices from the same view,  $\hat{y}_{1\sim n-1}^M = \{\hat{y}_1, \dots, \hat{y}_{n-1}\}^M$ . These capture the already-known information from earlier slices of the current view. Second,

*cross-view priors*, which consist of encoded slices from the opposite view,  $\hat{\mathbf{y}}_{1 \sim q}^M = \{\hat{\mathbf{y}}_1, \dots, \hat{\mathbf{y}}_q\}^M$ , where  $q = n - 1$  for  $M = L$  (left view) and  $q = n$  for  $M = R$  (right view). In other words, when encoding a left-view slice, we use all slices up to index  $n - 1$  from the right view as cross-view priors, and for a right-view slice we use up to index  $n$  from the left view. The HDC mechanism is applied to these cross-view priors to align them with the current view, compensating for disparity via disparity-aware shifting and cross-attention fusion. Third, spatial-temporal priors, which capture spatial and temporal context for the current slice, are denoted as  $\Phi_{1 \sim n}^M$ . These priors are obtained by fusing the hyperprior features with multi-scale context features ( $Ctx_{1 \sim 3}^M$ ), as illustrated in Fig. 3 (c). The spatial-temporal priors provide additional cues from the broader image context and temporal reference frames. By incorporating these three sets of priors,  $Est_n^M$  can more accurately estimate the probability distribution for  $\hat{\mathbf{y}}_n^M$ , leading to improved entropy modeling for that slice.

The entropy estimation process within  $Est_n^M$  is illustrated in Fig. 3 (b). First, the HDC mechanism performs cross-view alignment: it takes the available encoded slices from the opposite view  $\hat{\mathbf{y}}_{1 \sim q}^M$  and aligns them to the current view  $M$  using disparity compensation. This alignment uses spatial-temporal prior of the current view as an anchor to guide the disparity-aware shifting and cross-attention, following Sec. 3.2.1. However, unlike the earlier HDC-FER module, this alignment step omits any downsampling or upsampling operations and directly outputs the aligned cross-view priors (denoted as  $s_{1 \sim q}^M = \{s_1, \dots, s_q\}^M$ ).

Next, the entropy estimation network fuses the aligned cross-view priors with the intra-view and spatial-temporal priors for the current slice. In particular,  $s_{1 \sim q}^M$ ,  $\hat{\mathbf{y}}_{1 \sim n-1}^M$ , and  $\Phi_n^M$  are concatenated and processed by a dedicated convolutional module (a DepthConvBlock). This module outputs the parameters of a parametric probability distribution for the current latent slice, mean  $\mu_n^M$  and scale  $\sigma_n^M$ . Using these predicted parameters, the encoder then quantizes the input slice  $\mathbf{y}_n^M$  by subtracting the mean, rounding to the nearest integer, and adding the mean back:

$$\hat{\mathbf{y}}_n^M = \lfloor \mathbf{y}_n^M - \mu_n^M \rfloor + \mu_n^M, \quad (5)$$

where  $\lfloor \cdot \rfloor$  denotes rounding to the nearest integer. The resulting quantized slice  $\hat{\mathbf{y}}_n^M$  is stored and treated as a known prior for subsequent entropy estimation steps, enabling the encoding process to adapt progressively as more slices (and cross-view information) become available.

Overall, by integrating HDC-based cross-view alignment into the entropy model, the HDC-EM module yields more accurate probability estimates for each latent slice. This improvement in entropy modeling translates to fewer bits required for encoding, thereby enhancing overall compression efficiency.

### 3.3. Objective Function

We set the rate-distortion cost sum of the two views as optimization target like formal methods:

$$\mathcal{L}_t = \sum_{M \in \{L, R\}} \{\lambda d(\mathbf{x}_t^M, \hat{\mathbf{x}}_t^M) + r(\hat{\mathbf{y}}_t^M) + r(\hat{\mathbf{z}}_t^M)\}, \quad (6)$$

where  $M$  denotes the view,  $L$  or  $R$ ,  $d(\mathbf{x}_t^M, \hat{\mathbf{x}}_t^M)$  denotes the distortion between the original uncompressed frame  $\mathbf{x}_t^M$  and the reconstruction frame  $\hat{\mathbf{x}}_t^M$  at time step  $t$ , which is usually measured by MSE or MS-SSIM loss. The term  $r(\hat{\mathbf{y}}_t^M) + r(\hat{\mathbf{z}}_t^M)$  represents the total bit rate for representing transmission features in both motion and context compression.  $\lambda$  is a hyperparameter used to control the trade-off factor between the total bit rate and distortion, controlling the balance between transmitted information and reconstruction quality.

## 4. Experiments

### 4.1. Evaluation Datasets.

For evaluation, previous NSVC approaches [11, 24] primarily focused on autonomous driving datasets, such as Cityscapes [16] and KITTI [19, 46], limiting their assessments to this specific domain. To ensure a fair comparison, we follow their experimental settings for Cityscapes and KITTI, adopting the same frame selection and pre-processing. Furthermore, to evaluate performance beyond autonomous driving scenarios, we extend our experiments to the Nagoya dataset [3], which represents more general multi-view scenes.

**Cityscapes.** The Cityscapes dataset [16] comprises 2975, 500, and 1525 stereo sequences for training, validation, and testing, respectively. Each sequence contains 30 frames at a resolution of  $2048 \times 1024$ . Following [11, 24], we crop frames to  $1920 \times 704$  by removing the top, left, and bottom regions. We use the test set of Cityscapes to analyze performance, with the Group of Pictures (GOP) set to 30, matching the sequence length.

**KITTI.** The KITTI 2012 [19] and KITTI 2015 [46] datasets contain 195 and 200 stereo sequences, respectively, with each sequence comprising 21 frames. Following [11, 24], we crop frames to  $1216 \times 320$  for testing. The GOP is set to 21 for evaluation.

**Nagoya.** Unlike Cityscapes and KITTI, which focus on autonomous driving, the Nagoya dataset [3] provides general-scene multi-view video sequences. To assess the generalization capability of our model, we select two standard MV-HEVC benchmark sequences [53], Kendo and Balloons, from the Nagoya MPEG-FTV project [3]. We evaluate our method on the first 96 frames, using the first and third views from both sequences. The GOP is set to 32.

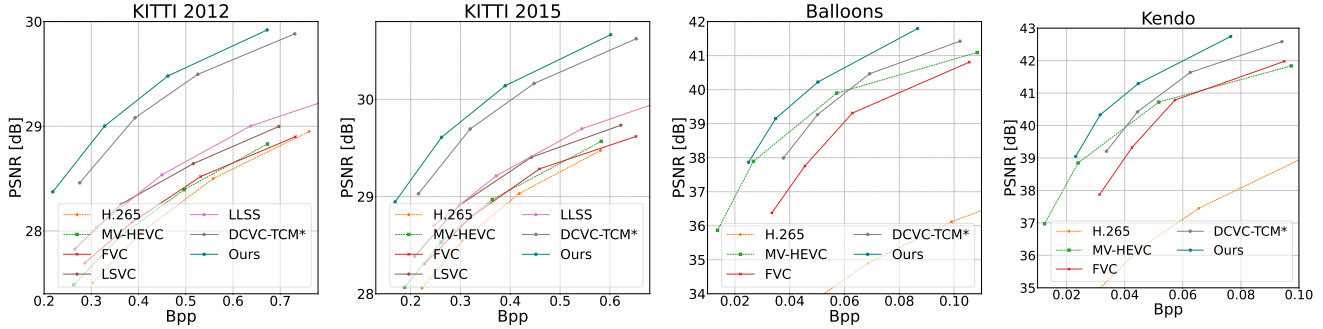


Figure 4. Rate-distortion curves. The results are evaluated on the KITTI 2012, KITTI 2015 and Nagoya [3] datasets in terms of Bpp-PSNR.

Method	Cityscapes	KITTI 2012	KITTI 2015	Kendo	Balloons
MV-HEVC [53]	0.0	0.0	0.0	0.0	0.0
HEVC [52]	34.14	7.77	12.64	314.281	515.20
FVC [27]	-14.9	-2.35	0.97	31.17	56.57
DCVC-TCM*	-24.17	-48.61	-46.82	-4.70	7.97
LSVC [11]	-32.05	-17.18	-13.47	—	—
LLSS [25]	-49.44	-18.18	-15.76	—	—
Ours	<b>-53.13</b>	<b>-55.97</b>	<b>-54.72</b>	<b>-27.96</b>	<b>-19.92</b>

Table 1. BD-rate (%) comparison in RGB colorspace measured with PSNR. The anchor is MV-HEVC.

## 4.2. Experiment Protocols

**Evaluation Metrics.** We evaluate image reconstruction quality using two widely adopted metrics: Peak Signal-to-Noise Ratio (PSNR) and Multi-Scale Structural Similarity Index Measure (MS-SSIM) [58]. Additionally, we measure compression efficiency using bits per pixel (Bpp). During compression, the first frame of each GOP (I-frame) is encoded using the learned image compression model proposed by He et al. [23], while subsequent frames (P-frames) are compressed using our method.

**Implementation Details.** We train four models, each corresponding to a different rate-distortion trade-off, determined by the Lagrange multiplier  $\lambda$  ( $\lambda = 256, 512, 1024, 2048$ ). The training process includes pre-training a single-view variant of our model on the Vimeo-90K dataset [63] and then finetuning on the Cityscapes dataset [16] following previous methods [11, 25]. Further details of training procedures and hyperparameters are provided in Sec. A in the appendix.

## 4.3. Comparison with State-of-the-art Methods

**Baseline Methods.** Following previous works [11, 25], we compare our model with various single-view and stereo video compression methods, including traditional codecs, neural-based video compression baselines, and state-of-the-art NSVC approaches. Specifically, we evaluate against traditional methods HEVC [52], MV-HEVC [53] and neural-based video compression methods FVC [27], as well as

neural-based stereo video compression methods LSVC [11] and LLSS [25].

For traditional baselines, we use the HM-16.20 [1] implementation with the `lowdelay_P_main` preset for HEVC and the HTM-16.3 [2] implementation with the `baseCfg_2view` configuration for MV-HEVC. The results for HEVC, MV-HEVC, FVC, LSVC, and LLSS on the Cityscape [16] and KITTI [19, 46] datasets are obtained via email correspondence with the authors, ensuring consistency with previous comparisons.

Additionally, we compare with DCVC-TCM\*, a computationally efficient variant of DCVC-TCM [50] and the backbone of our framework. DCVC-TCM\* reduces complexity by using fewer channels and a lighter motion estimation network [54], while preserving its core architecture. Our framework extends DCVC-TCM\* by integrating HDC-FER and HDC-EM, further improving compression efficiency. For fair evaluation, DCVC-TCM\* follows the same training pipeline described in Sec. 4.2, with pretraining on Vimeo-90K [63] and fine-tuning on Cityscapes [16].

**Rate-Distortion Performance.** The rate-distortion (RD) curves in Fig. 4 compare our proposed method against baseline approaches in terms of Bpp-PSNR across four datasets: KITTI 2012 [19], KITTI 2015 [46], and the Kendo and Balloons video sequences from the Nagoya dataset [3]. As the figure illustrates, our model consistently achieves state-of-the-art performance across all datasets, demonstrating a significant improvement in rate-distortion efficiency

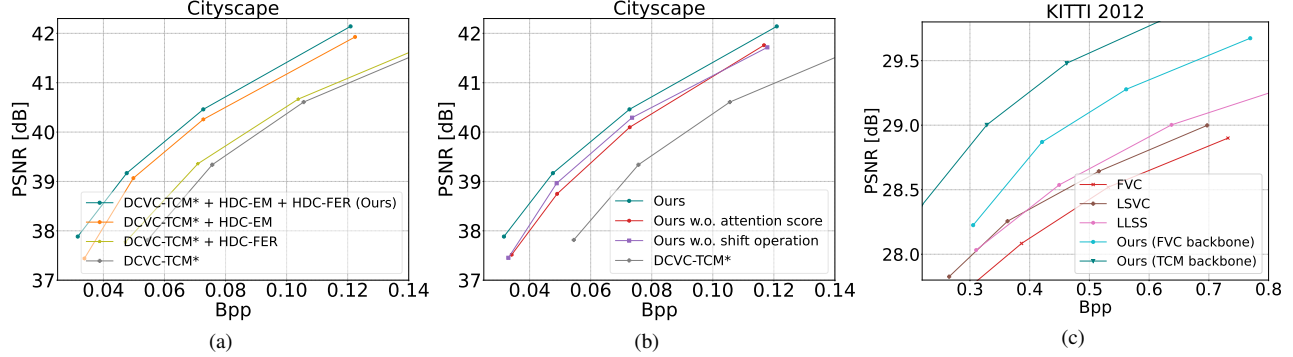


Figure 5. (a) and (b) present the ablation studies of our proposed modules on the Cityscapes dataset [16]. (c) shows the comparison with previous SOTA NSVCs (LSVC [11] and LLSS [25]) under the same backbone on the KITTI 2012 dataset [19].

over existing methods. LSVC and LLSS are not included in the comparison on Kendo and Balloons due to the unavailability of their pretrained models.

Tab. 1 provides a detailed quantitative analysis using BD-Rate [8] as the evaluation metric, calculated based on Bpp-PSNR with MV-HEVC [53] as the anchor. On the autonomous driving datasets (*i.e.*, Cityscapes, KITTI 2012, and KITTI 2015), our method achieves an average BD-rate saving of approximately 54.61% compared to the anchor MV-HEVC, and around 26.81% compared to the previous SOTA NSVC method LLSS. We would also like to emphasize that on general-scene multi-view video sequences (*i.e.*, Kendo and Balloons), our method achieves an average BD-rate saving of approximately 23.91% compared to the anchor MV-HEVC, and outperforms our single-view baseline DCVC-TCM\* by about 24.54% on average. This demonstrates the superiority of exploiting disparity redundancy in indoor stereo scenes, whereas previous NSVC methods (*e.g.*, LSVC and LLSS) typically only showcase such benefits in auto-driving scenarios. The results indicate that our proposed approach outperforms traditional and neural-based stereo video codecs, achieving lower BD-Rate values across all four datasets. Performance comparisons using MS-SSIM as the distortion metric and a model complexity analysis of the proposed method against baseline methods are detailed in Sec. B and Sec. C of the appendix.

#### 4.4. Ablation Study

**Effectiveness of HDC-FER and HDC-EM.** To evaluate the individual and combined effectiveness of our proposed HDC-FER and HDC-EM modules, we conduct an ablation study based on the single-view baseline model DCVC-TCM\* using the Cityscapes dataset. Specifically, the variant DCVC-TCM\* + HDC-FER integrates HDC-FER modules into the feature extraction and reconstruction process of the baseline method DCVC-TCM\*, enabling enhanced feature representation during the encoding and decoding stages to simultaneously compress the two views of stereo frames. DCVC-TCM\* + HDC-EM replaces the original single view

entropy module of DCVC-TCM\* with the proposed cross-view HDC-EM entropy model, which leverages information from both views to achieve more accurate entropy estimation for each view in an autoregressive manner. The results presented in Fig. 5 (a) demonstrate that integrating HDC-FER alone (DCVC-TCM\* + HDC-FER) achieves a BD-rate reduction of 6.03%, and substituting the entropy module with HDC-EM (DCVC-TCM\* + HDC-EM) results in a BD-rate reduction of 26.59%. When both modules are simultaneously integrated into the model (DCVC-TCM\* + HDC-EM + HDC-FER), the total BD-rate reduction is further improved to 32.17%, thereby confirming the significant benefits of employing cross-view information and enhanced feature representation for compression performance.

**Effectiveness on Implicit and Explicit Compensation in HDC.** To validate the effectiveness of the implicit and explicit compensation within our HDC mechanism, we conduct an ablation study on the Cityscapes dataset, focusing on the “attention score” (*i.e.*, implicit cross-attention) and the shift operation (*i.e.*, explicit pixel displacement). First, removing the “attention score” from both HDC-EM and HDC-FER modules results in cross-view features being extracted solely from the shifted feature volumes, without the guidance of attention weighting. As shown in Fig. 5 (b), this modification leads to a 13.75% increase in BD-rate, highlighting the significant role of the implicit cross-attention mechanism in improving compression efficiency. Next, to assess the contribution of explicit pixel displacement, we disable the shift operation in both modules, thereby allowing feature interaction between views only through simple channel attention. This results in a 9.08% increase in BD-rate, as illustrated in Fig. 5 (b), demonstrating the effectiveness of explicit pixel displacement in facilitating cross-view feature extraction.

**Effectiveness of Single-View NVC Backbone.** To rigorously assess the effectiveness of the proposed HDC-FER and HDC-EM modules, we take the KITTI 2012 dataset as an example to perform a controlled comparison by integrating them into the same backbone architecture as prior

SOTA NVC methods, including LSVC [11] and LLSS [25]. Concretely, we start from the official pretrained FVC [27] model trained on the Vimeo-90K dataset [63], incorporate our modules into its framework, and finetune the resulting model on Cityscapes [16], following the protocol detailed in Sec. 4.2.

As presented in Fig. 5 (c), our method achieves superior performance over prior SOTA approaches under identical backbone settings, thereby substantiating the contribution of the proposed modules to compression efficiency. Moreover, when employing DCVC-TCM\* as the backbone—which corresponds to the final configuration of our model—further performance gains are observed, reaffirming the scalability and general applicability of the proposed HDC-FER and HDC-EM modules.

## 5. Conclusion

In this work, we propose a novel neural stereo video compression (NSVC) framework that integrates a hybrid disparity compensation (HDC) strategy to effectively reduce cross-view redundancy. By combining explicit pixel displacement for structural priors with implicit cross-attention mechanisms for flexible feature alignment, HDC enhances both disparity compensation accuracy and optimization efficiency. We further incorporate HDC into two key modules: HDC-FER for cross-view feature extraction and reconstruction, and HDC-EM for cross-view entropy modeling, enabling more effective compression. Extensive experiments on both autonomous driving and general multi-view datasets demonstrate that our framework outperforms previous neural and traditional stereo video compression methods, highlighting its superiority in both efficiency and reconstruction quality.

## References

- [1] HEVC test model (hm). <https://hevc.hhi.fraunhofer.de/>. Accessed: 2024-10-26. 7
- [2] MV-HEVC test model (htm). <https://hevc.hhi.fraunhofer.de/>. Accessed: 2024-10-26. 7
- [3] Nagoya university sequences. <https://www.fujii.nuee.nagoya-u.ac.jp/multiview-data/>. Accessed: 2025-2-26. 2, 6, 7, 1
- [4] Eirikur Agustsson, David Minnen, Nick Johnston, Johannes Balle, Sung Jin Hwang, and George Toderici. Scale-space flow for end-to-end optimized video compression. In *Proceedings of the IEEE/CVF Conference on Computer Vision and Pattern Recognition*, pages 8503–8512, 2020. 2
- [5] Johannes Ballé, Valero Laparra, and Eero P Simoncelli. End-to-end optimized image compression. *arXiv preprint arXiv:1611.01704*, 2016. 2
- [6] Johannes Ballé, David Minnen, Saurabh Singh, Sung Jin Hwang, and Nick Johnston. Variational image compression with a scale hyperprior. *arXiv preprint arXiv:1802.01436*, 2018. 2
- [7] Fabrice Bellard. Bpg image format. <https://bellard.org/bpg/>. Accessed: 2024-10-26. 2
- [8] G Bjontegaard. Calculation of average psnr differences between rd-curves. *ITU-T SG16 Q*, 6, 2001. 8, 1
- [9] Benjamin Bross, Ye-Kui Wang, Yan Ye, Shan Liu, Jianle Chen, Gary J Sullivan, and Jens-Rainer Ohm. Overview of the versatile video coding (vvc) standard and its applications. *IEEE Transactions on Circuits and Systems for Video Technology*, 31(10):3736–3764, 2021. 2
- [10] Zhenghao Chen, Shuhang Gu, Guo Lu, and Dong Xu. Exploiting intra-slice and inter-slice redundancy for learning-based lossless volumetric image compression. *IEEE Transactions on Image Processing*, 31:1697–1707, 2022. 2
- [11] Zhenghao Chen, Guo Lu, Zhihao Hu, Shan Liu, Wei Jiang, and Dong Xu. Lsvc: A learning-based stereo video compression framework. In *Proceedings of the IEEE/CVF Conference on Computer Vision and Pattern Recognition*, pages 6073–6082, 2022. 1, 2, 3, 6, 7, 8, 9
- [12] Zhenghao Chen, Lucas Relic, Roberto Azevedo, Yang Zhang, Markus Gross, Dong Xu, Luping Zhou, and Christopher Schroers. Neural video compression with spatio-temporal cross-covariance transformers. In *Proceedings of the 31st ACM International Conference on Multimedia*, pages 8543–8551, 2023. 2
- [13] Zhenghao Chen, Luping Zhou, Zhihao Hu, and Dong Xu. Group-aware parameter-efficient updating for content-adaptive neural video compression. In *Proceedings of the 32nd ACM International Conference on Multimedia*, pages 11022–11031, 2024. 2
- [14] Zhengxue Cheng, Heming Sun, Masaru Takeuchi, and Jiro Katto. Learned image compression with discretized gaussian mixture likelihoods and attention modules. In *Proceedings of the IEEE/CVF conference on computer vision and pattern recognition*, pages 7939–7948, 2020. 2, 5
- [15] Xiaojie Chu, Liangyu Chen, and Wenqing Yu. Nafssr: Stereo image super-resolution using nafnet. In *Proceedings of the IEEE/CVF conference on computer vision and pattern recognition*, pages 1239–1248, 2022. 1, 2
- [16] Marius Cordts, Mohamed Omran, Sebastian Ramos, Timo Rehfeld, Markus Enzweiler, Rodrigo Benenson, Uwe Franke, Stefan Roth, and Bernt Schiele. The cityscapes dataset for semantic urban scene understanding. In *Proceedings of the IEEE conference on computer vision and pattern recognition*, pages 3213–3223, 2016. 6, 7, 8, 9, 1
- [17] Xin Deng, Wenzhe Yang, Ren Yang, Mai Xu, Enpeng Liu, Qianhan Feng, and Radu Timofte. Deep homography for efficient stereo image compression. In *Proceedings of the IEEE/CVF Conference on Computer Vision and Pattern Recognition*, pages 1492–1501, 2021. 1, 2, 3
- [18] Abdelaziz Djelouah, Joaquim Campos, Simone Schaub-Meyer, and Christopher Schroers. Neural inter-frame compression for video coding. In *Proceedings of the IEEE/CVF international conference on computer vision*, pages 6421–6429, 2019. 2
- [19] Andreas Geiger, Philip Lenz, and Raquel Urtasun. Are we ready for autonomous driving? the kitti vision benchmark suite. In *2012 IEEE conference on computer vision and pattern recognition*, pages 3356–3363, 2012. 2

tern recognition, pages 3354–3361. IEEE, 2012. 2, 6, 7, 8, 1

[20] Xiaoyang Guo, Kai Yang, Wukui Yang, Xiaogang Wang, and Hongsheng Li. Group-wise correlation stereo network. In *Proceedings of the IEEE/CVF conference on computer vision and pattern recognition*, pages 3273–3282, 2019. 1, 2

[21] Minghao Han, Shiyin Jiang, Shengxi Li, Xin Deng, Mai Xu, Ce Zhu, and Shuhang Gu. Causal context adjustment loss for learned image compression. *arXiv preprint arXiv:2410.04847*, 2024. 2

[22] Tao Han, Zhenghao Chen, Song Guo, Wanghan Xu, and Lei Bai. Cra5: Extreme compression of era5 for portable global climate and weather research via an efficient variational transformer. *arXiv preprint arXiv:2405.03376*, 2024.

[23] Dailan He, Ziming Yang, Weikun Peng, Rui Ma, Hongwei Qin, and Yan Wang. Elic: Efficient learned image compression with unevenly grouped space-channel contextual adaptive coding. In *Proceedings of the IEEE/CVF Conference on Computer Vision and Pattern Recognition*, pages 5718–5727, 2022. 2, 5, 7, 1

[24] Yung-Han Ho, Chih-Peng Chang, Peng-Yu Chen, Alessandro Gnutti, and Wen-Hsiao Peng. Canf-vc: Conditional augmented normalizing flows for video compression. In *European Conference on Computer Vision*, pages 207–223. Springer, 2022. 2, 6

[25] Qiqi Hou, Farzad Farhadzadeh, Amir Said, Guillaume Sautiere, and Hoang Le. Low-latency neural stereo streaming. In *Proceedings of the IEEE/CVF Conference on Computer Vision and Pattern Recognition*, pages 7974–7984, 2024. 1, 2, 3, 4, 7, 8, 9

[26] Zhihao Hu, Zhenghao Chen, Dong Xu, Guo Lu, Wanli Ouyang, and Shuhang Gu. Improving deep video compression by resolution-adaptive flow coding. In *Computer Vision–ECCV 2020: 16th European Conference, Glasgow, UK, August 23–28, 2020, Proceedings, Part II 16*, pages 193–209. Springer, 2020. 2

[27] Zhihao Hu, Guo Lu, and Dong Xu. Fvc: A new framework towards deep video compression in feature space. In *Proceedings of the IEEE/CVF Conference on Computer Vision and Pattern Recognition*, pages 1502–1511, 2021. 7, 9, 2

[28] Zhihao Hu, Guo Lu, Jinyang Guo, Shan Liu, Wei Jiang, and Dong Xu. Coarse-to-fine deep video coding with hyperprior-guided mode prediction. In *Proceedings of the IEEE/CVF Conference on Computer Vision and Pattern Recognition*, pages 5921–5930, 2022. 2

[29] Alex Kendall, Hayk Martirosyan, Saumitro Dasgupta, Peter Henry, Ryan Kennedy, Abraham Bachrach, and Adam Bry. End-to-end learning of geometry and context for deep stereo regression. In *Proceedings of the IEEE international conference on computer vision*, pages 66–75, 2017. 1, 2, 3, 4

[30] Diederik P Kingma. Adam: A method for stochastic optimization. *arXiv preprint arXiv:1412.6980*, 2014. 1

[31] Jianjun Lei, Xiangrui Liu, Bo Peng, Dengchao Jin, Wanqing Li, and Jingxiao Gu. Deep stereo image compression via bi-directional coding. In *Proceedings of the IEEE/CVF Conference on Computer Vision and Pattern Recognition*, pages 19669–19678, 2022. 1, 3

[32] Han Li, Shaohui Li, Wenrui Dai, Chenglin Li, Junni Zou, and Hongkai Xiong. Frequency-aware transformer for learned image compression. *arXiv preprint arXiv:2310.16387*, 2023. 2

[33] Jiahao Li, Bin Li, and Yan Lu. Deep contextual video compression. *Advances in Neural Information Processing Systems*, 34:18114–18125, 2021. 2

[34] Jiahao Li, Bin Li, and Yan Lu. Hybrid spatial-temporal entropy modelling for neural video compression. In *Proceedings of the 30th ACM International Conference on Multimedia*, pages 1503–1511, 2022.

[35] Jiahao Li, Bin Li, and Yan Lu. Neural video compression with diverse contexts. In *Proceedings of the IEEE/CVF Conference on Computer Vision and Pattern Recognition*, pages 22616–22626, 2023.

[36] Jiahao Li, Bin Li, and Yan Lu. Neural video compression with feature modulation. In *Proceedings of the IEEE/CVF Conference on Computer Vision and Pattern Recognition*, pages 26099–26108, 2024.

[37] Bowen Liu, Yu Chen, Rakesh Chowdary Machineni, Shiyu Liu, and Hun-Seok Kim. Mmvc: Learned multi-mode video compression with block-based prediction mode selection and density-adaptive entropy coding. In *Proceedings of the IEEE/CVF Conference on Computer Vision and Pattern Recognition*, pages 18487–18496, 2023. 2

[38] Jerry Liu, Shenlong Wang, and Raquel Urtasun. Dsic: Deep stereo image compression. In *Proceedings of the IEEE/CVF International Conference on Computer Vision*, pages 3136–3145, 2019. 1, 2, 3

[39] Jinming Liu, Heming Sun, and Jiro Katto. Learned image compression with mixed transformer-cnn architectures. In *Proceedings of the IEEE/CVF conference on computer vision and pattern recognition*, pages 14388–14397, 2023. 2, 5

[40] Lei Liu, Zhihao Hu, Zhenghao Chen, and Dong Xu. Icmh-net: Neural image compression towards both machine vision and human vision. In *Proceedings of the 31st ACM International Conference on Multimedia*, pages 8047–8056, 2023.

[41] Lei Liu, Zhenghao Chen, Zhihao Hu, and Dong Xu. An efficient adaptive compression method for human perception and machine vision tasks. *arXiv preprint arXiv:2501.04329*, 2025. 2

[42] Zhenling Liu, Xinjie Zhang, Jiawei Shao, Zehong Lin, and Jun Zhang. Bidirectional stereo image compression with cross-dimensional entropy model. *arXiv preprint arXiv:2407.10632*, 2024. 3

[43] Guo Lu, Wanli Ouyang, Dong Xu, Xiaoyun Zhang, Chunlei Cai, and Zhiyong Gao. Dvc: An end-to-end deep video compression framework. In *Proceedings of the IEEE/CVF conference on computer vision and pattern recognition*, pages 11006–11015, 2019. 2

[44] Guo Lu, Chunlei Cai, Xiaoyun Zhang, Li Chen, Wanli Ouyang, Dong Xu, and Zhiyong Gao. Content adaptive and error propagation aware deep video compression. In *Computer Vision–ECCV 2020: 16th European Conference, Glasgow, UK, August 23–28, 2020, Proceedings, Part II 16*, pages 456–472. Springer, 2020. 1

[45] Fabian Mentzer, George Toderici, David Minnen, Sung-Jin Hwang, Sergi Caelles, Mario Lucic, and Eirikur Agustsson. Vct: A video compression transformer. *arXiv preprint arXiv:2206.07307*, 2022. 2

[46] Moritz Menze and Andreas Geiger. Object scene flow for autonomous vehicles. In *Proceedings of the IEEE conference on computer vision and pattern recognition*, pages 3061–3070, 2015. 2, 6, 7, 1

[47] David Minnen and Saurabh Singh. Channel-wise autoregressive entropy models for learned image compression. In *2020 IEEE International Conference on Image Processing (ICIP)*, pages 3339–3343. IEEE, 2020. 2

[48] Diganta Misra. Mish: A self regularized non-monotonic activation function. *arXiv preprint arXiv:1908.08681*, 2019. 4

[49] Zhelun Shen, Yuchao Dai, Xibin Song, Zhibo Rao, Dingfu Zhou, and Liangjun Zhang. Pcw-net: Pyramid combination and warping cost volume for stereo matching. In *European conference on computer vision*, pages 280–297. Springer, 2022. 1, 2, 3, 4

[50] Xihua Sheng, Jiahao Li, Bin Li, Li Li, Dong Liu, and Yan Lu. Temporal context mining for learned video compression. *IEEE Transactions on Multimedia*, 25:7311–7322, 2022. 2, 3, 7, 1

[51] Athanassios Skodras, Charilaos Christopoulos, and Touradj Ebrahimi. The jpeg 2000 still image compression standard. *IEEE Signal processing magazine*, 18(5):36–58, 2001. 2

[52] Gary J Sullivan, Jens-Rainer Ohm, Woo-Jin Han, and Thomas Wiegand. Overview of the high efficiency video coding (hevc) standard. *IEEE Transactions on circuits and systems for video technology*, 22(12):1649–1668, 2012. 2, 7

[53] Gerhard Tech, Ying Chen, Karsten Müller, Jens-Rainer Ohm, Anthony Vetro, and Ye-Kui Wang. Overview of the multiview and 3d extensions of high efficiency video coding. *IEEE Transactions on Circuits and Systems for Video Technology*, 26(1):35–49, 2015. 1, 2, 6, 7, 8

[54] Zachary Teed and Jia Deng. Raft: Recurrent all-pairs field transforms for optical flow. In *Computer Vision–ECCV 2020: 16th European Conference, Glasgow, UK, August 23–28, 2020, Proceedings, Part II 16*, pages 402–419. Springer, 2020. 7, 2

[55] Anthony Vetro, Thomas Wiegand, and Gary J Sullivan. Overview of the stereo and multiview video coding extensions of the h. 264/mpeg-4 avc standard. *Proceedings of the IEEE*, 99(4):626–642, 2011. 1, 2

[56] Longguang Wang, Yingqian Wang, Zhengfa Liang, Zaiping Lin, Jungang Yang, Wei An, and Yulan Guo. Learning parallax attention for stereo image super-resolution. In *Proceedings of the IEEE/CVF conference on computer vision and pattern recognition*, pages 12250–12259, 2019. 1, 2

[57] Yingqian Wang, Xinyi Ying, Longguang Wang, Jungang Yang, Wei An, and Yulan Guo. Symmetric parallax attention for stereo image super-resolution. In *Proceedings of the IEEE/CVF Conference on Computer Vision and Pattern Recognition*, pages 766–775, 2021. 1, 2

[58] Zhou Wang, Eero P Simoncelli, and Alan C Bovik. Multiscale structural similarity for image quality assessment. In *The Thirly-Seventh Asilomar Conference on Signals, Systems & Computers*, 2003, pages 1398–1402. Ieee, 2003. 7

[59] Thomas Wiegand, Gary J Sullivan, Gisle Bjontegaard, and Ajay Luthra. Overview of the h. 264/avc video coding standard. *IEEE Transactions on circuits and systems for video technology*, 13(7):560–576, 2003. 2

[60] Matthias Wödlinger, Jan Kotera, Jan Xu, and Robert Sablatnig. Sasic: Stereo image compression with latent shifts and stereo attention. In *Proceedings of the IEEE/CVF Conference on Computer Vision and Pattern Recognition*, pages 661–670, 2022. 1, 2, 3

[61] Matthias Wödlinger, Jan Kotera, Manuel Keglevic, Jan Xu, and Robert Sablatnig. Ecsic: Epipolar cross attention for stereo image compression. In *Proceedings of the IEEE/CVF Winter Conference on Applications of Computer Vision*, pages 3436–3445, 2024. 1, 3

[62] Yueqi Xie, Ka Leong Cheng, and Qifeng Chen. Enhanced invertible encoding for learned image compression. In *Proceedings of the 29th ACM international conference on multimedia*, pages 162–170, 2021. 2

[63] Tianfan Xue, Baian Chen, Jiajun Wu, Donglai Wei, and William T Freeman. Video enhancement with task-oriented flow. *International Journal of Computer Vision*, 127:1106–1125, 2019. 7, 9, 1

[64] Yongqi Zhai, Luyang Tang, Yi Ma, Rui Peng, and Ronggang Wang. Disparity-based stereo image compression with aligned cross-view priors. In *Proceedings of the 30th ACM International Conference on Multimedia*, pages 2351–2360, 2022. 1, 3

[65] Shengping Zhang, Wei Yu, Feng Jiang, Liqiang Nie, Hongxun Yao, Qingming Huang, and Dacheng Tao. Stereo image restoration via attention-guided correspondence learning. *IEEE Transactions on Pattern Analysis and Machine Intelligence*, 46(7):4850–4865, 2024. 1, 2

[66] Xinjie Zhang, Jiawei Shao, and Jun Zhang. Ldmic: Learning-based distributed multi-view image coding. *arXiv preprint arXiv:2301.09799*, 2023. 1, 3

[67] Renjie Zou, Chunfeng Song, and Zhaoxiang Zhang. The devil is in the details: Window-based attention for image compression. In *Proceedings of the IEEE/CVF conference on computer vision and pattern recognition*, pages 17492–17501, 2022. 2

# Appendix

In the appendix, we provide additional details and experimental results to further support our framework. Section **A** describes the training strategy and experimental settings for both training and testing. Section **B** presents an extended rate-distortion analysis using BD-rate measured with MS-SSIM. To evaluate computational efficiency, Section **C** compares the FLOPs and parameter counts of our method with baseline approaches. Finally, Section **D** details the network architecture, including the integration of HDC-FER and HDC-EM into the motion and context compression modules.

## A. Detailed Training and Testing Settings

**Training Strategy.** Our training process consists of four stages. First, following DCVC-TCM [50], we pretrain a single-view variant of our model on the Vimeo-90K dataset [63], excluding all HDC-FER modules and cross-view priors in entropy modeling. We then progressively incorporate our proposed HDC-FER and HDC-EM modules into the model while fine-tuning it on the Cityscapes dataset [16] using the Adam optimizer [30] with a batch size of 4 and a learning rate of  $1 \times 10^{-5}$ . Throughout training, we optimize the cascaded distortion loss [44]  $D_{\text{rec}}^*$ , and the rate loss,  $R_{\text{all}}^*$  over four consecutive P-frames, preserving gradients across these frames. The full training strategy is outlined in Table **S2**.

In Stage 2, we introduce cross-view priors into the entropy model by integrating HDC-EM and fine-tune for 300k iterations. In Stage 3, HDC-FER modules are incorporated and pretrained for 20k iterations while keeping other components fixed. Finally, in Stage 4, the full model (with both HDC-EM and HDC-FER) undergoes an additional 200k iterations of fine-tuning.

To optimize for MS-SSIM, we further fine-tune the model trained with MSE for an additional 100k iterations, replacing the distortion loss with  $1 - \text{MS-SSIM}(\mathbf{x}_t^M, \hat{\mathbf{x}}_t^M)$ , improving performance under the MS-SSIM metric.

**Training Settings** Following prior works [11, 25], we optimize our model using MSE and MS-SSIM as distortion metrics. The loss function is defined as  $\text{MSE}(\mathbf{x}_t^M, \hat{\mathbf{x}}_t^M)$  for MSE optimization and  $1 - \text{MSSSIM}(\mathbf{x}_t^M, \hat{\mathbf{x}}_t^M)$  for MS-SSIM optimization.

For I-frame compression, we employ the learned image compression model ELIC [23], fine-tuning it on the Cityscapes [16] training set for 200 epochs with a batch size of 8. The rate-distortion trade-off parameter  $\lambda$  is set to  $\{0.008, 0.016, 0.016, 0.15\}$  for MSE-based training and  $\{3, 12, 12, 40\}$  for MS-SSIM-based training.

For P-frame training, we pretrain our model on Vimeo-90K [63] using randomly cropped into  $256 \times 256$ . In later

training stages, Cityscapes frames are cropped to  $256 \times 384$ . To enhance model generalization, we apply random horizontal and vertical flipping as data augmentation.

**Testing Settings.** We follow the preprocessing procedures of prior works [11, 25] for evaluating on Cityscapes [16], KITTI 2012 [19], and KITTI 2015 [46]. For Cityscapes, we crop 64 pixels from the top, 256 pixels from the bottom, and 128 pixels from the left to remove rectification artifacts and the ego vehicle, resulting in a resolution of  $1920 \times 704$ . For the KITTI 2012 and KITTI 2015 datasets, frames are cropped to a size of  $1216 \times 320$  by removing pixels from the top and left. Additionally, we exclude video sequences 000127 and 000182 from KITTI 2012, and 000026 and 000167 from KITTI 2015 to maintain consistency with prior studies. For the newly introduced dataset Nagoya [3], no cropping is applied, and frames are kept at the original  $1024 \times 768$  resolution.

## B. BD-rate measured by bpp-MS-SSIM

We evaluate performance using MS-SSIM as the distortion metric, calculating BD-rate [8] with MV-HEVC [53] as the anchor. The results, presented in Table **S3**, show that our method outperforms all baseline approaches, achieving the best performance in terms of Bpp-MS-SSIM.

## C. Model complexity

Table **S4** compares the FLOPs and parameter counts of our model with DCVC-TCM [50], DCVC-TCM\*, LSVC [11], and LLSS [25], using a  $512 \times 512$  input frame pair. The FLOPs and parameter values for LLSS are taken from its published work, while LSVC values were provided by the authors. We measured FLOPs and parameters for DCVC-TCM, DCVC-TCM\*, and our method on an NVIDIA RTX 4090 GPU.

As shown in Table **S4**, DCVC-TCM\*, a modified version of DCVC-TCM (our backbone model), reduces FLOPs from 735G to 431G, significantly lowering computational complexity. Integrating the proposed HDC-FER and HDC-EM modules into DCVC-TCM\* slightly increases FLOPs to 536.90G while still maintaining a substantially lower computational cost than DCVC-TCM. Compared to previous SOTA NSVC methods LSVC and LLSS, our model achieves superior compression performance with significantly reduced computational overhead. These results highlight the computational efficiency and effectiveness of HDC-FER and HDC-EM, making our method suitable for deployment in resource-constrained environments.

## D. Network Structure

Our network consists of five key components: motion estimation, motion compression, motion compensation, con-

Stage	P Frames	Network	Loss	LR	Iterations
Stage 2	4	All (Add cross-view priors)	$D_{rec}^* \& R_{all}^*$	1e-5	3e5
Stage 3	4	HDC-FER modules	$D_{rec}^* \& R_{all}^*$	1e-5	2e4
Stage 4	4	The full model	$D_{rec}^* \& R_{all}^*$	1e-5	2e5

Table S2. Training strategy

Method	Cityscapes	KITTI 2012	KITTI 2015	Kendo	Balloons
MV-HEVC [53]	0.0	0.0	0.0	0.0	0.0
HEVC [52]	34.37	14.23	16.96	238.97	1449.67
FVC [27]	-30.96	-40.83	-35.34	—	—
DCVC-TCM* [33]	-35.13	-48.86	-38.46	-42.02	26.05
LSVC [11]	-46.88	-51.60	-47.20	—	—
LLSS [25]	-58.10	-55.71	-51.16	—	—
Ours	<b>-58.95</b>	<b>-60.03</b>	<b>-51.19</b>	<b>-55.49</b>	<b>-8.84</b>

Table S3. BD-rate (%) comparison in RGB colorspace measured with MS-SSIM. The anchor is MV-HEVC.

Method	Params(M)	FLOPs(G)
DCVC-TCM [50]	10.55	735.95
DCVC-TCM*	9.68	431.24
LSVC [11]	50.50	1760.0
LLSS [25]	39.22	634.9
Ours	16.39	536.90

Table S4. Model complexity comparison. \* denotes our reproduced baseline model.

text compression, and frame reconstruction. For motion estimation, we adopt a lightweight version of RAFT [54], initialized with official pretrained weights. The motion compensation and frame reconstruction modules follow the structures of DEVC-TCM [50], with a reduced number of channels to lower model complexity.

We further detail the motion and context compression modules, where our proposed HDC-FER and HDC-EM modules are integrated. Specifically, HDC-FER is incorporated into the encoder, decoder, hyper-encoder, and hyper-decoder of both motion and context compression networks. Meanwhile, HDC-EM acts as the entropy model, performing entropy prediction for both modules. The structures of the motion and context compression networks are illustrated in Fig. S6.

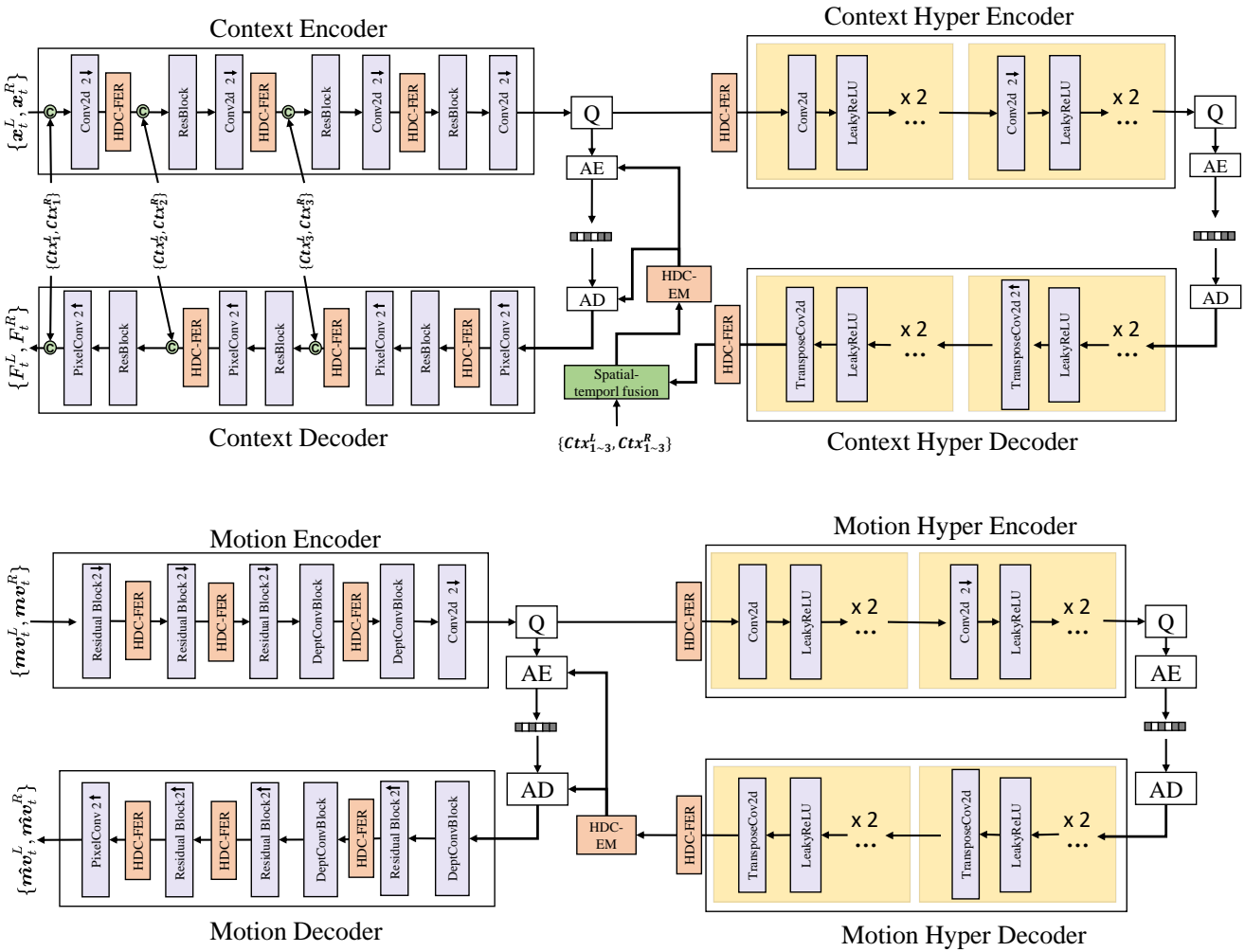


Figure S6. The structure of motion and context compression network